Heliyon 7 (2021) e06827

Contents lists available at ScienceDirect

Heliyon

journal homepage: www.cell.com/heliyon

Research article

Electronic and optical properties' tuning of phenoxazine-based D-A_2-π-A_1 organic dyes for dye-sensitized solar cells. DFT/TDDFT investigations

Samson Olusegun Afolabi [a], Banjo Semire [b], Mopelola Abidemi Idowu [a,*]

[a] Department of Chemistry, Federal University of Agriculture, P.M.B. 2240, Abeokuta, Nigeria
[b] Department of Pure and Applied Chemistry, Ladoke Akintola University of Technology, Ogbomoso, Nigeria

ARTICLE INFO

Keywords:
DFT
Phenoxazine
Donor subunit
Bathochromic shift
V_{oc}

ABSTRACT

Modulation of molecular features of metal free organic dyes is important to present sensitizers with competing electronic and optical properties for dye sensitized solar cells (DSSCs). The D-A_2-π-A_1 molecular design based on phenothiazine skeleton (D) connected with benzothiadiazole (A_2) linked with furan π-spacer and acceptor unit of cynoacrylic acid (A_1) were fabricated and examined theoretically for possible use as DSSCs. Density functional theory (DFT) and time dependent density functional theory TDDFT were used to study the effect of additional donors on the photophysical properties of the dyes. Eight (8) different donor subunits were introduced at C7 of phenoxazine based dye skeleton to extend the π-conjugation, lower HOMO-LUMO gap (E_g) and improve photocurrent efficiency of the dye sensitizer. All the dye sensitizers (except P3 and P4) exhibited capability of injecting electrons into the conduction band of the semiconductor (TiO_2) and regenerated via redox potential (I^-/I_3^-) electrode. Attachment of 2-hexylthiophene (P2) remarkably lowered the E_g, extended π-electron delocalization, hence, gives higher absorption wavelength (λ_{max}) at 752 nm. The donor subunit containing 2-hexylthiophene (P2) presented the best chemical hardness, open circuit voltage (V_{oc}), and other comparable electronic properties, making P2 the best DSSC candidate amongst the optimized dyes. The reported dyes would be interesting for further experimental research.

1. Introduction

The necessity of photovoltaics as a substantial source of energy cannot be overemphasized. An increase in the world population contributes immensely to high energy demand, and though fossil fuel has been the most prominent source of energy, it has limitations of global warming and environmental pollution [1, 2, 3]. Therefore, the solar cell becomes imperative to curb threats posed to human health and the environment by fossil fuel. The solar cell is an appliance that converts sunlight to electrical energy [4]. Solar energy has advantages of being clean, cheap, renewable, inexhaustible, pollution-free, and large-scale production [5]. Since the sun has more than enough energy that can be consumed for a million years, then solar energy remains a pivotal source of energy.

For about three decades, the research into dye-sensitized solar cells (DSSCs) has been intense due to its flexibility, low production cost and biodegradability [6,7]. The five components of DSSCs include a mesoporous oxide semiconductor layer, a transparent conducting glass substrate, redox electrolyte, a counter electrode and a dye sensitizer [8,9]. However, dye sensitizer plays the foremost role of light absorption, stability, charge separation, charge injection, conversion of incident light into photocurrent, light-harvesting efficiency and the overall power conversion efficiency [10, 11, 12]. A suitable sensitizer must have a broad solar spectrum for high photocurrent [11]. At the same time, the lowest unoccupied molecular orbital (LUMO) level of dyes must be higher than the energy conduction band (E_{CB}) of the semiconductor electrode and the highest occupied molecular orbital (HOMO) level must be lower than the redox potential of the electrolyte [11, 12, 13].

Majorly, there are two types of sensitizers; metal-free organic dyes and metal complex sensitizers. Researches have shown that the DSSCs based on metal-complex sensitizers exhibit slightly higher efficiency than those of metal-free organic sensitizers [6, 7, 8, 9, 10, 11, 12, 13]. However, the metal-complex sensitizers have limited resources, low molar extinction coefficient and high cost, which limit their industrial applications [12,14]. Studies have revealed that metal-free organic sensitizers provide better performance than metal complexes' sensitizers because of higher molar extinction coefficients, tunable spectral responses, ease of production and availability [9,10,13,15].

* Corresponding author.
E-mail address: maidowu408@yahoo.com (M.A. Idowu).

https://doi.org/10.1016/j.heliyon.2021.e06827
Received 19 June 2020; Received in revised form 13 December 2020; Accepted 13 April 2021

Many metal-free organic dyes including phenothiazine [14], carbazoles, coumarin, triarylamines, triphenylamine [16, 17, 18, 19, 20, 21, 22, 23], or phenoxazine [24, 25, 26, 27] have been designed and synthesized and found to possess promising properties that can enhance photovoltaic performances better than most prominent metal complex dyes. In recent times, phenoxazine has shown preference as an electron-donating moiety. Karlsson and coworkers [26] affirmed that phenoxazine display higher conversion efficiencies than triphenylamine and phenothiazine-based dyes with a similar structure. Moreover, the challenges of lower conversion efficiency, narrow absorption spectra, poor stability and poor photovoltaic properties peculiar to metal-free organic dyes can be overcome with the flexibility of phenoxazine, by lowering the energy bandgap through the incorporation of additional donor groups into the molecular moiety [28,29].

Higher oxidation potential and lower aromatic energy of furan as π-spacer has been reported to aid stability of the dye and improve power conversion efficiency [30] amongst many other π-spacers such as pyrrole, thiazole, benzene or thiophene used in the study of organic dyes [14,25, 31]. According to Buene and co-workers [32], furan π-spacer performed better than popular π -spacers such as thiophene and phenyl, therefore the use of furan as π-spacer is encouraged to facilitate intramolecular charge transfer from donor to acceptor [14]. The acceptor group can perform the function of an electron trap and also an anchor group [14,15, 25,27]. Cyanoacrylic acid is regarded as an excellent electron acceptor owing to its excellent electron withdrawing ability [33] compared to various reported acceptor groups such as benzothiadiazole or 2-cyano-2--pyran-4-ylidene-acetic acid [14,30].

Several architectural designs such as D-A, D-π-A, D-A-π-A [11,14,30, 31], have helped in the design of many highly efficient organic dyes. Absorption spectra of D-A and D-π-A structured organic dyes were found to be narrow, which is not beneficial for higher short-circuit current density [14,17]. To broaden the absorption band, one strategy is to decrease the E_g by employing a stronger electron donor [34]. Compared to D-π-A dyes, the properties of D-A-π-A organic dyes maybe adjusted by inserting an auxiliary acceptor between the D and π units, thereby providing more flexible photoelectric properties [17]. This method would not only enhance electron mobility from donor unit to anchor group but also modulate the energy level spectrum and light response region [35].

Studies have shown that Density Functional theory (DFT) methods are helpful to describe the ground state features and also provide accurate results in the analysis of the electronic properties of many-electron systems [36, 37, 38]. Time-Dependent DFT (TDDFT) shares the same concept of DFT. This method has been extensively used for the study of excited states of DSSC dyes, both for the isolated molecule and for the molecule attached to the semiconductor surface [39]. Several works have reported that DFT and TDDFT methods are capable of estimating photoelectric features of different dyes [12, 13, 14, 15, 16].

This paper adopts a D-A_2-π-A_1 design, Figure 1a using the phenoxazine-based ring as electron-donating unit, while benzothiadiazole (A_2) was introduced between electron donor and π-spacer as 'electron trap' tool to fine-tune the HOMO-LUMO gap, broaden the light-harvesting range and promote the electron transfer from donor to anchor [14]. Furan was employed as a π-conjugated bridge to enhance intramolecular charge transfer [25,32]. Cyanoacrylic acid is pivotal in anchoring the dye into the semiconductor and improving cell efficiency [15]. Eight (8) additional donor units were developed (Figure 1b) to enhance the effective donation of electrons from donor to anchor group. Each donor subunit was introduced at the C7 point of phenoxazine-based dye ring to study the effects of donor subgroup on electronic properties of the dye and develop new dyes with improved performance in DSSCs employing DFT and TDDFT methods.

(a)

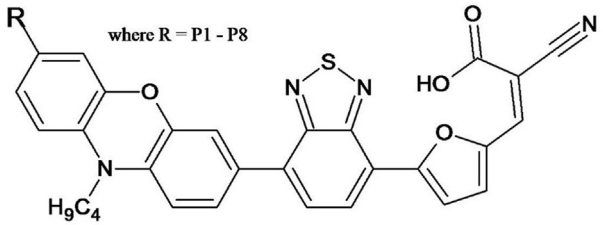

(b)

Dye	Structure	Name	Dye	Structure	Name
P1	H	Hydrogen	P5	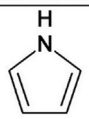	Pyrrole
P2	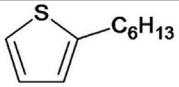	2-hexylthiophene	P6	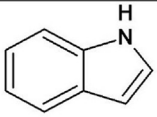	Indole
P3	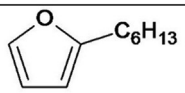	2-hexylfuran	P7	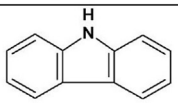	Carbazole
P4	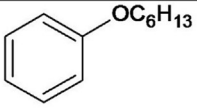	(hexyloxy)benzene	P8	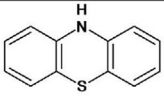	Phenothiazine

Figure 1. (a) Molecular structure of the simulated dyes (b) donor subunits attached to C7 of the simulated dyes.

2. Computational methods

Geometrical design and optimization of the sensitizers (P1–P8) was within the graphical user interface of Spartan 14. Frequency analyses were performed to obtain the lowest energy geometries. No imaginary frequency was observed from the results proving that all the geometries are at a global minimum. Optimization of the ground state of the sensitizers was carried out in the gas phase using DFT level of theory with three-parameter density functional, which includes Becke's gradient exchange correction and the Lee, Yang, Parr correlation functional (B3LYP) at 6-31G** standard basis set [40]. Polarized split-valence 6-31G** was proved to be sufficient and give reliable results [41,42]. The HOMO-1, HOMO, LUMO, and LUMO+1 levels were calculated together with their electron density. This gave access to the easy calculation of molecular orbital and energies. The chemical reactivity parameters such as chemical hardness, electrophilicity index, electrodonating power, and electroaccepting power were calculated using DFT conceptual as reported by Delgado-Montiel [43,44]. The UV-Vis spectra of the geometries were evaluated using TD-DFT with B3LYP and 6-31G** theory [23,45] using conductor like polarizable continuum solvation model in the gas phase; which is considered sufficient for the prediction of absorption spectra [46,47]. The λ_{max} and oscillator strength were obtained from the systems. The light harvesting efficiency (LHE) was obtained by the oscillator strength of the highest λ_{max}. The suitability of the molecules was ranked based on their HOMO-LUMO energy gap. The dye with the lowest E_g (P2), having required HOMO and LUMO energies, was further optimized using B3LYP/6-31G* and B3LYP/6-31+G* level of theory. This was done to prove the reliability of the results. All the dyes were designed and optimized on an Intel Core i5, 2.6 GHZ machine to investigate the effect of various electron donating subgroups on electronic and optical properties of phenoxazine-based dyes to improve the light-to-current efficiency of the dyes. All the computations were executed on Spartan 14 software by wavefunction Inc [48].

3. Results and discussion

Geometrical properties (dihedral angle and bond length) from the optimized structures Figure 2 were analyzed and the most representative are presented in Table 1 (the Cartesian coordinates of the optimized structures of the phenoxazine-based dyes are displayed in the supplementary material). Dihedral angle reveals the angle betwixt two planes. The dihedral angles within the optimized molecules were between (a) the donor subunit (D_0) and a donor unit (D) identified as (φD_0-D_1), (b) the donor unit (D) and electron trap (A_2), tagged as (φD-A_2), (c) the electron trap (A_2) and the π-bridge unit (π), represented by (φA_2-π); and (d) the π-bridge unit (π) and the acceptor unit (A_1), assigned as (φπ-A). The dihedral angle is substantial in intramolecular charge transfer [49]. The impact of the donor subunits on the dihedral angles were studied to get an insight into the probability of intramolecular charge transfer. Considering the dihedral angle of P1–P4, the φD-A_2 dihedral angle of P1 is -30.21°, the introduction of 2-hexylthiophene in P2 decreased the φD-A_2 dihedral angle by 1.34°. When the 2-hexylthiophene was replaced by 2-hexylfuran to give P3, the φD-A_2 decreased further by 2.59° in comparison with P1. Attachment of hexyloxybenzene to P1 to generate P4 also decreased the dihedral angle by 1.38°. A decrease in dihedral angles observed in P2, P3 and P4 can be attributed to the strong electron withdrawing ability of sulphur and oxygen heteroatoms on the additional electron donating unit [50]. Furthermore, pyrrole, indole, carbazole, and phenothiazine (donor subunits) were attached to P1 to give P5, P6, P7 and P8 respectively; linked at the C7 point of the phenoxazine ring with a nitrogen atom. This imparts a high φD_0-D_1 dihedral angle between the chemical groups and phenoxazine. Looking at φD-A_2 dihedral angles of

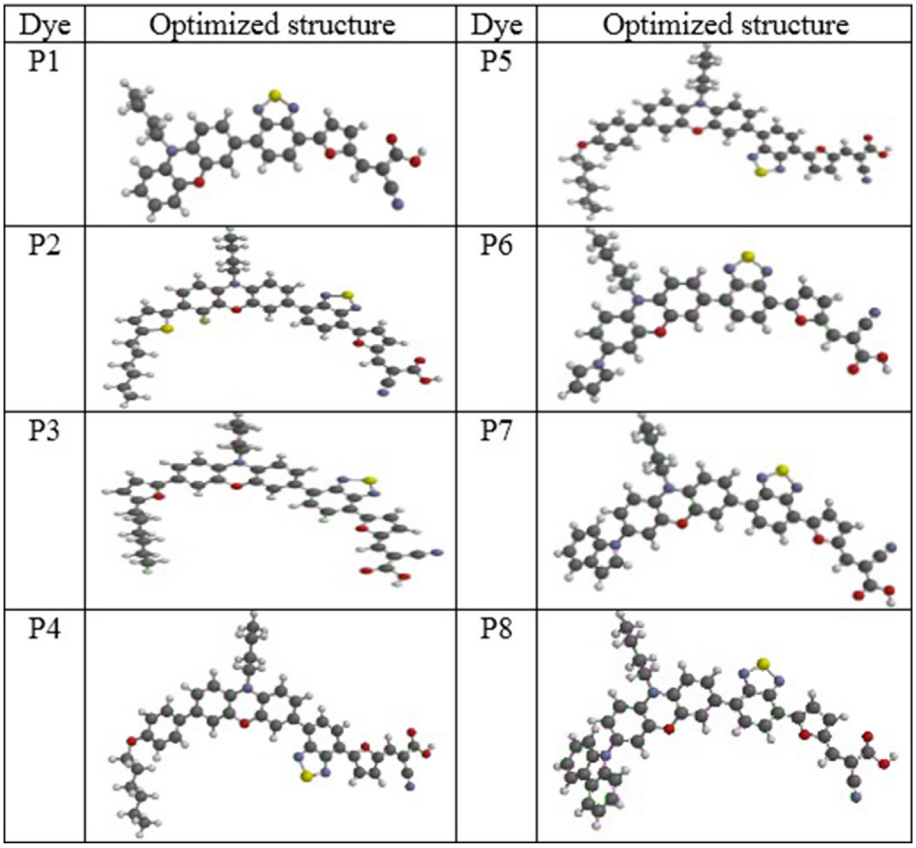

Figure 2. Calculated optimized geometries of phenoxazine based dyes.

Table 1. Selected dihedral angles and bond lengths of the simulated molecules.

Dye	Parameter	ϕD_0-D_1	Parameter	ϕD-A_2	Parameter	$\phi A_2.\pi$	Parameter	$\phi\pi$-A_1
P1	-	-	C–C–C–C C–C	-30.21° 1.472Å	C–C–C–S C–C	-0.65° 1.445Å	S–C–C–C C–C	-179.94° 1.417Å
P2	S–C–C–C C–C	26.94° 1.464Å	C–C–C–C C–C	-28.87° 1.472Å	C–C–C–S C–C	0.31° 1.445Å	S–C–C–C C–C	179.95° 1.418Å
P3	O–C–C–C C–C	-1.39° 1.454Å	C–C–C–C C–C	-27.62° 1.471Å	C–C–C–S C–C	0.01° 1.445Å	S–C–C–C C–C	-179.24° 1.416Å
P4	C–C–C–C C–C	34.58° 1.481Å	C–C–C–C C–C	-28.83° 1.472Å	C–C–C–S C–C	-0.53° 1.445Å	S–C–C–C C–C	-179.24° 1.416Å
P5	C–N–C–C C–C	-36.10° 1.415Å	C–C–C–C C–C	-30.18° 1.472Å	C–C–C–S C–C	-0.37° 1.445Å	S–C–C–C C–C	-179.74 1.416Å
P6	C–N–C–C C–C	45.15° 1.416Å	C–C–C–C C–C	-28.83° 1.472Å	C–C–C–S C–C	-0.88° 1.445Å	S–C–C–C C–C	-179.93° 1.416Å
P7	C–N–C–C C–C	57.36° 1.419Å	C–C–C–C C–C	-30.52° 1.472Å	C–C–C–S C–C	-0.46° 1.445Å	S–C–C–C C–C	-179.86° 1.418Å
P8	C–N–C–C C–C	82.83° 1.436Å	C–C–C–C C–C	-30.26° 1.473Å	C–C–C–S C–C	-0.03° 1.445Å	S–C–C–C C–C	179.86° 1.417Å

these systems, Table 1, P6 with indole subunit possess the lowest dihedral angle (-28.83°) which is suitable for intramolecular charge transfer. The $\varphi A_2.\pi$ dihedral angle of the molecules enhances charge transfer from electron trap moieties (A_2) to the π-conjugated bridge, while $\varphi\pi$-A_1 dihedral angles are also beneficial for charge transfer from a π-conjugated bridge to acceptor group (A_1), thus, higher possibility of injection of electron from the dye into the semiconductor. It can be concluded that auxiliary donors improve the planarity of P2–P6, as well as electron transportation from donor to acceptor. The bond distances did not present significant variations among the dyes (as shown in Table 1).

3.1. Frontier molecular orbitals

Studies have shown frontier molecular orbitals also called HOMO and LUMO are related to intramolecular charge transfer behavior and have a great effect on the electronic excitation and absorption spectra [13,51]. The HOMO energy level is related to the oxidation potential of the dye sensitizer, where high oxidation potential results in a high driving force for the reduction of the oxidized dye [7,52] whereas the LUMO is electrophilic and electron accepting. Generally, the HOMO of a strong dye-sensitizer is mainly localized on the donor unit while the LUMO is localized on the acceptor unit [7]. The orbital spatial distributions and the compositions of the HOMO–1, HOMO, LUMO, and LUMO+1 for these dyes are displayed in Figure 3. The electron density in the HOMO of P1 to P7 dyes spread over phenoxazine and additional donors. Contrarily, the HOMO of P8 was mainly localized on the phenothiazine donor subgroup. This can result from a higher dihedral angle (φD_0-D_1) between phenothiazine and phenoxazine. This predicts a decrease in intramolecular charge transfer between the donor subunit and phenoxazine which can cause low oscillator strength [53]. Molecular orbital distribution of HOMO-1 mainly delocalized across the rings except for P5 to P7 which were mainly populated by donor subgroup. This can be attributed to the S-character of nitrogen atom which is more electronegative than p-character hence holds electron tightly [54]. The molecular orbital distribution of LUMO and LUMO+1 of the dyes spread across the benzothiadiazole, π-spacer and acceptor group. So, a change of electron density is favourable for electron injection from the dye molecule to the semiconductor [5,14].

3.2. The natural bond orbital (NBO) population analysis

The NBO charges were calculated from the optimized dye structures in the ground state to elucidate delocalization of the electron density and intramolecular charge transfer mechanism [31,55] of D-A_2-π-A_1 dyes as shown in Table 2. Since an additional donor was used to enrich the electron donating group, the duo was taken as a donor unit. For the electron donating group, the positive charge shows an effective electron donor unit. However, the donor group (D) of P3 exhibits a negative charge, thus, behaves as an electron withdrawing group due to the strong electronegativity of the oxygen atom on 2-hexyl furan. The negative charge on the acceptor group indicates that electrons are well trapped from the electron donating unit and electron acceptor unit. The NBO results reveal that all the simulated dyes except P3 favour NBO charge transfer from donor to acceptor units through the help of benzothiadiazole and π-spacer, thus behaves as D-A_2-π-A_1.

3.3. Molecular electrostatic potential (MEP)

The MEP is an alternative approach to understand the electrostatic contribution of charge distribution of molecules in three dimensions [56]. It also reveals molecular sizes, shapes, charge densities, and electrostatic potential reactive sites in the molecules [57]. The MEP of the designed dyes was determined from the optimized molecules in their ground state as shown in Figure 4. Its surface appears in different colours (blue, red, yellow, or green), blue as positive extreme and red as negative [58]. The blue region which corresponds to the positive electrostatic potential or electron-deficient region is localized on the hydrogen atom while the red or yellow colour that represents a negative electrostatic potential or electron-rich area is mainly situated on the acceptor moiety. The green colour observed signifies zero potential region [57,58]. The colour of electrostatic potential can be sequenced as red < orange < yellow < green < blue [57]. This confirms the effective intramolecular charge transfer between the donor to the acceptor unit [59].

3.4. Energy HOMO-LUMO gap

The electronic properties of the optimized dyes were further studied to understand the possibilities of electron injection into the semiconductor and regeneration of dye via redox potential. The E_g is one of the crucial parameters that determine the suitability of a dye for DSSC application [26]. Thus, E_g can be expressed as in Eq. (1) [58,60].

$$E_g = E_{LUMO} - E_{HOMO} \quad (1)$$

where E_{LUMO} and E_{HOMO} are the energies associated with the lowest unoccupied molecular orbital and the highest occupied molecular orbital respectively.

Low HOMO-LUMO gap encourages bathochromic shift and in turn, improves photovoltaic efficiency [51]. Figure 5 reveals the E_g of HOMO-1, HOMO, LUMO, and LUMO+1 energy levels of the optimized dyes. P1 is a non-donor subgroup on the C7 and possess E_g of 1.97 eV. The additional donors were introduced to lower E_g and improve photocurrent efficiencies of organic dyes with attachment of 2-hexylthiophene,

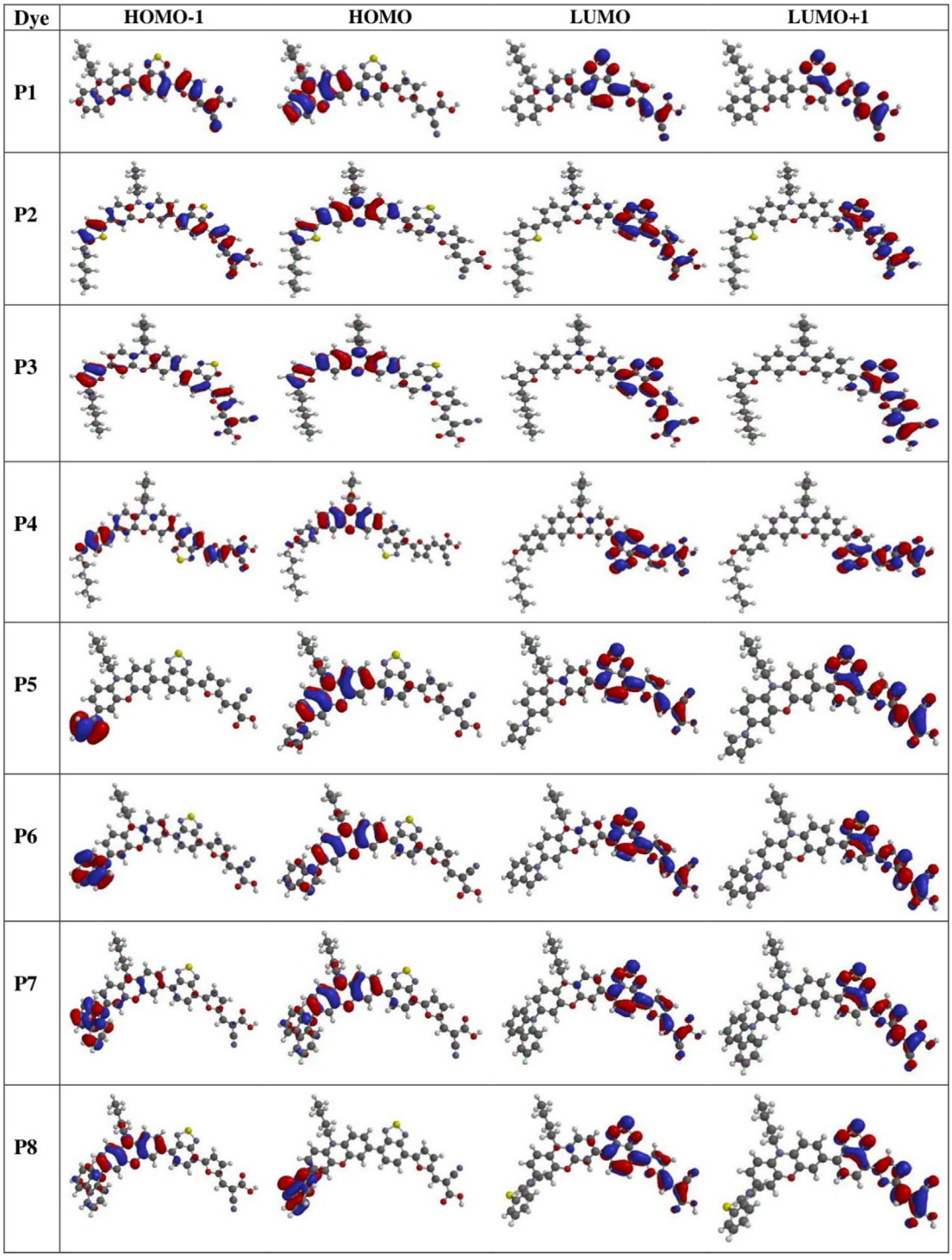

Figure 3. Frontier molecular orbitals of the simulated dyes.

2-hexylfuran, and hexyloxybenzene into C7 point of P1 to give P2, P3, and P4 respectively. The HOMO, LUMO and E_g of these dyes are (-4.94, -2.97, 1.97 eV), (-4.82, -2.97, 1.85 eV) (-4.74, -2.94, 1.80 eV) and (-4.79, -2.94, 1.85 eV). It is noted that the introduction of each substituent destabilized the HOMO value by 0.12, 0.20 and 0.15 eV respectively compared to P1. The LUMO values of P3 and P4 were also destabilized by 0.03 eV, whereas, 2-hexylthiophene on P2 has no effect on LUMO value compared to P1. This phenomenon led to their low E_g. As it is observed, the introduction of the three-donor subgroup lowers the E_g by 0.12, 0.17, and 0.12 eV.

Furthermore, a series of nitrogen atom containing compounds such as pyrrole, indole, carbazole, and phenothiazine were attached to P1 to give P5–P8. The introduction of pyrrole and indole has no effect on the HOMO value of P5 and P6 but increases their LUMO/E_g values by 0.03 and 0.05

Table 2. Total Charge Population Density of the studied dyes.

Dye	D	A	Π	A
P1	0.125	-0.073	0.182	-0.233
P2	0.114	-0.073	0.182	-0.233
P3	-0.087	-0.072	0.168	-0.218
P4	0.124	-0.072	0.166	-0.219
P5	0.114	-0.064	0.168	-0.215
P6	0.110	-0.064	0.168	-0.215
P7	0.110	-0.060	0.171	-0.221
P8	0.110	-0.062	0.170	-0.213

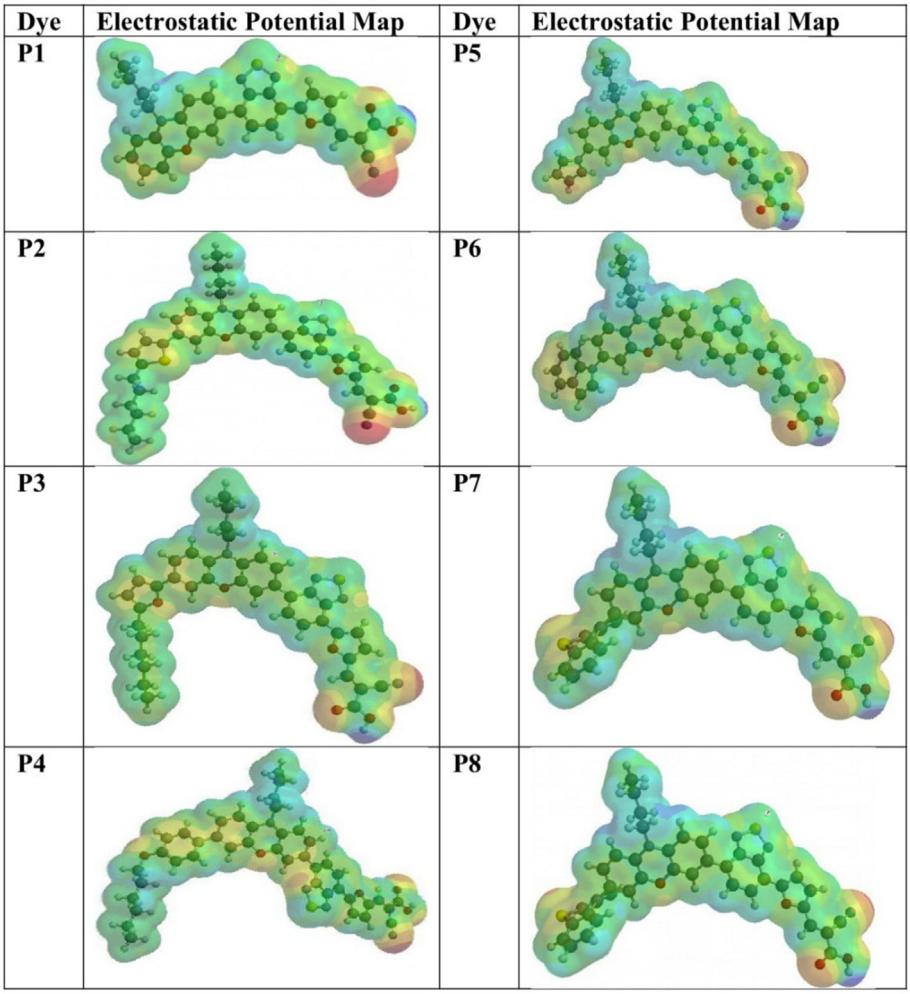

Figure 4. Molecular electrostatic potential maps for the simulated dyes.

eV respectively. A strong electron donating unit shifts the HOMO level more negative [61]. Observing the HOMO, LUMO and E_g of P7 (-5.00, -3.03, 1.97) and P8 (-5.00, -3.05, 1.95 eV), the HOMO/LUMO value of P7 were stabilized by 0.7/0.06 eV generating E_g of 1.97 eV. The HOMO of P8 was stabilized while the LUMO value was destabilized giving E_g of 1.95 eV.

A suitable dye sensitizer must have a HOMO value that is lower than the redox potential of I^-/I_3^- electrolyte which is -4.8 eV to enhance dye restoration by getting an electron from the electrolyte [62]. At the same time, the LUMO value of a suitable sensitizer should be above the conduction band of TiO_2 which is -4.0 eV [11,62] for the proper injection of an electron into the conduction band of the semiconductor. This reveals that all the simulated dyes are capable of injecting electrons into the conduction band of TiO_2 and restored by getting electrons from the redox potential of the electrolyte except P3 and P4 with unfavorable -4.74 and -4.79 eV HOMO value. The poor photovoltaic performance of these dyes is traceable to the strong electronegativity of the oxygen atom on the 2-hexylfuran ring and hexyloxybenzene which hold electrons to itself.

Li et al. [13] reported that apart from HOMO→ LUMO electronic transition, HOMO-1→LUMO and HOMO→LUMO+1 transition can also result in bathochromic shift especially when the energy of HOMO-1 and LUMO+1 are close to HOMO and LUMO respectively, due to extension of conjugation [7]. Figure 5 also shows the energy differences between HOMO-1 and LUMO for the P1–P8 dyes 2.85, 2.74, 2.68, 2.75, 2.75, 2.53, 2.49 and 2.09 eV respectively. Also, their energy differences between HOMO and LUMO+1 are 2.68, 2.57, 2.50, 2.55, 2.68, 2.66, 2.70 and 2.67

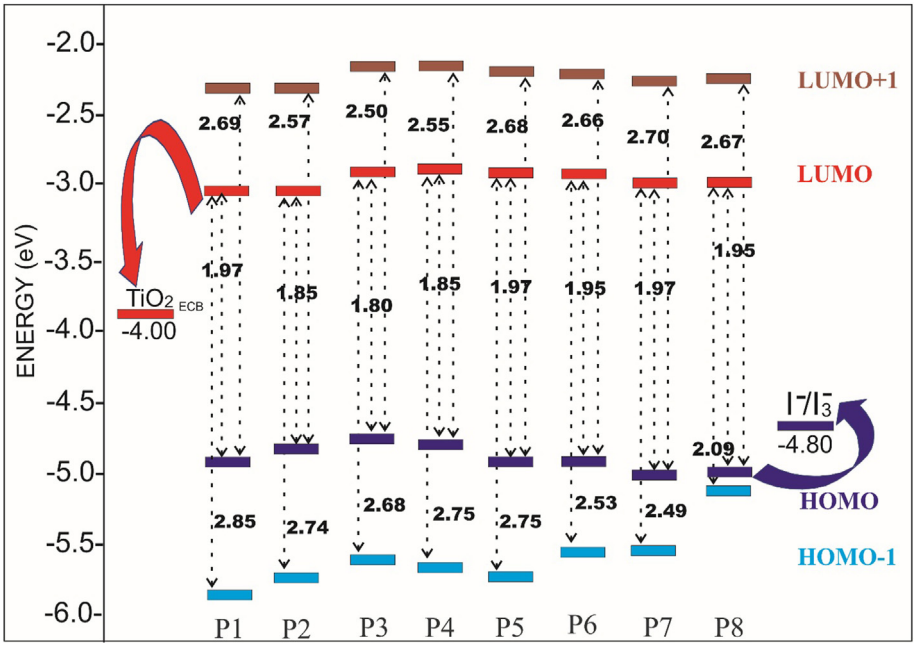

Figure 5. The electronic bandgap of the dye molecules.

eV accordingly. This suggests that the introduction of donor subgroup into the phenoxazine based backbone has a significant effect on energy level which possibly impart alteration of absorption spectra of the simulated dyes.

3.5. Absorption wavelength

The ultraviolet-visible absorption wavelength (λ_{max}) calculations were performed at TD-DFT/B3LYP/6-31G** level to understand the electronic transitions of the studied dyes. The conductor like polarizable continuum model (C-PCM) in the gas phase was the solvation model employed. Since the improvement of absorbed dyes could probably result in good LHE [52,63], thus absorption in the visible and near-ultraviolet (UV) region of the spectrum is crucial for light-to-current conversion [13,60]. Also, low E_g is essential to produce higher λ_{max} and increase the efficiency of DSSCs. Listed in Table 3 are singlet → singlet transitions of absorption bands with wavelength longer than 300 nm.

The absorption wavelength of P1– P8 are 703.78, 752.30, 777.12, 757.65, 707.89, 715.16, 710.93 and 715.95 nm respectively (Table 3). The absorption spectra of the molecules differ due to the effect of the donor subunit. Among the simulated dyes, P1 has the lowest absorption wavelength due to the absence of a conjugated donor subunit at the C7 point to initiate a bathochromic shift in comparison to other dyes. The redshift observed in P2–P8 compared to P1 is connected with the additional donor unit which delocalized electron conjugation within the molecule to cause a bathochromic shift. It is noted that the addition of 2-hexylthiophene and oxygen containing donor subunits; 2-hexylfuran and hexyloxybenzene in P2, P3 and P4 respectively, enhanced the delocalization of electron and thereby shifted the absorption band to longer wavelengths compared to P1 by 48.52, 73.34, and 53.87 nm respectively. Also, P5–P8 absorbed to longer wavelength by 4.11, 11.38, 7.15 and 12.17 nm respectively in comparison to P1. Due to the unmatched HOMO energies of P3 and P4 for a good sensitizer, as explained earlier, P2 is considered to exhibit the longest wavelength. It can be concluded that 2-hexylthiophene possesses high optical and structural stability to expand the absorption wavelength of the dye sensitizer [31]. All the sensitizers possess HOMO-LUMO molecular orbital showing π-π* transition with over 96% orbital contribution.

Among the eight simulated dyes, P2–P4 poses the lowest E_g and highest absorption wavelength. Meanwhile, the HOMO values of P3 and P4 do not meet the requirement for electron restoration in DSSC. Thus, P2 is regarded as the best dye for DSSC amongst the simulated dyes. To prove the reliability of the results, other basis set such as 6-31G* and 6–31 + G* were further employed on P2 as stated in Table 4. The E_g obtained from the two basis sets are 1.86 and 1.83 eV. This differs by 0.01 and 0.02 eV from 1.85 eV obtained using 6-31G**. Therefore, optimization of P2 using an additional basis set shows no significant changes in the result obtained using 6-31G**.

In 2016, Zhang and co-workers [14] reported phenothiazine-based dyes with D-A-π-A design (PTZ-1), where benzothiadiazole served as electron modulator and phenyl ring was employed as π-spacer, and cyanoacetic acid was used as an electron acceptor. The E_g and absorption wavelength of this molecule are 2.37 eV and 463 nm respectively. Similarly, Wu and Zhu [64] reported WS-1 and WS-3 with E_g and absorption wavelength (2.06 eV, 496 nm) and (2.28 eV, 455 nm) respectively. Comparing these results with P1, it is expected that P1 will outperform PTZ-1 or WS-1 due to better E_g (1.97 eV) which is necessary for higher absorption wavelength (703.78 nm). Improvement noticed in P1 is traceable to good electron donating ability of phenoxazine compared to phenothiazine aided by electron transport enhancement of furan π-bridge.

3.6. Predicted photovoltaic properties

The prediction of overall photoelectric conversion efficiency can be estimated as in Eq. (2) [65];

$$\eta = \frac{J_{SC} \times V_{oc} \times ff}{P} \tag{2}$$

where J_{sc} = short circuit current density, V_{oc} = open circuit voltage, ff = fill factor, P = intensity of the incident light. The fill factor can be described by Eq. (3) [7].

$$ff = \frac{I_m \times V_m}{J_{SC} \times V_{oc}} \tag{3}$$

While I_m and V_m are current and voltage related to maximum power. Eq. (3) reveals that the photoelectric conversion efficiency of photovoltaic is mainly related to ff, J_{sc}, and V_{oc}. However, J_{sc} [14] can be calculated following Eq. (4).

Table 3. Calculated absorption peak (λ_{max}), oscillator strength (f) and electronic transition and LHE for phenoxazine based dyes at TD-DFT/B3LYP/6-31G** level of theory.

Dye	λ_{max}	f	Electronic Transition	LHE
P1	355.65	0.0770	HOMO → LUMO+2 69% HOMO-3 → LUMO 19%	0.16
	372.40	0.7517	HOMO-1 → LUMO+1 48% HOMO-3 → LUMO 18% HOMO → LUMO+2 13% HOMO-2 → LUMO 10%	0.82
	397.72	0.0458	HOMO-2 → LUMO 81%	0.10
	454.13	0.7602	HOMO-1 → LUMO 76%	0.83
	523.23	0.0030	HOMO → LUMO+1 89%	0.01
	703.78	0.5226	HOMO → LUMO 97%	**0.70**
P2	385.31	0.2245	HOMO → LUMO+2 71% HOMO-3 → LUMO 22%	0.40
	397.56	0.3744	HOMO-1→ LUMO+1 41% HOMO-3 → LUMO 39% HOMO → LUMO+2 13%	0.58
	452.17	0.3661	HOMO-2 → LUMO 76%	0.57
	477.63	0.4389	HOMO-1 → LUMO 76%	0.64
	542.61	0.0027	HOMO → LUMO+1 91%	0.01
	752.30	0.4937	HOMO → LUMO 98%	**0.68**
P3	384.92	0.2164	HOMO → LUMO+2 68% HOMO-3 → LUMO 26%	0.39
	401.70	0.3840	HOMO-1→ LUMO+1 55% HOMO-3 → LUMO 29%	0.59
	454.40	0.4911	HOMO-2 → LUMO 76%	0.68
	495.20	0.3081	HOMO-1 → LUMO 81%	0.51
	559.75	0.0037	HOMO → LUMO+1 93%	0.01
	777.12	0.4604	HOMO → LUMO 98%	**0.65**
P4	380.60	0.5493	HOMO → LUMO+2 51% HOMO-3 → LUMO 22% HOMO-1 → LUMO+1 21%	0.72
	399.41	0.1809	HOMO-3 → LUMO 55% HOMO-1 → LUMO+1 35%	0.34
	455.90	0.6189	HOMO-2 → LUMO 71%	0.76
	481.14	0.2389	HOMO-1 → LUMO 77% HOMO-2 → LUMO 18%	0.42
	549.91	0.0051	HOMO → LUMO+1 93%	0.01
	757.65	0.4927	HOMO → LUMO 97%	**0.68**
P5	387.04	0.3592	HOMO-4 → LUMO 47% HOMO-2 → LUMO+1 44%	0.56
	419.51	0.0068	HOMO-3 → LUMO 95%	0.02
	454.63	0.7555	HOMO-2 → LUMO 79%	0.82
	523.85	0.0025	HOMO → LUMO+1 90%	0.01
	707.89	0.5265	HOMO → LUMO 97%	**0.70**
P6	406.71	0.2046	HOMO-1 → LUMO+1 89%	0.38
	445.05	0.1932	HOMO-3 → LUMO 87%	0.36
	458.32	0.4530	HOMO-2 → LUMO 79%	0.65
	519.83	0.0397	HOMO → LUMO+1 69% HOMO-1 → LUMO 21%	0.09
	536.28	0.0725	HOMO-1 → LUMO 77% HOMO → LUMO+1 22%	0.15
	715.16	0.5007	HOMO → LUMO 98%	**0.68**
P7	411.66	0.2124	HOMO-1 → LUMO+1 89%	0.39
	453.15	0.6061	HOMO-3 → LUMO 73%	0.75
	514.27	0.0154	HOMO → LUMO+1 85%	0.03
	548.16	0.1231	HOMO-1 → LUMO 93%	0.25
	710.93	0.4608	HOMO → LUMO 98%	**0.65**
P8	443.79	0.0108	HOMO-3 → LUMO 99%	0.02
	447.82	0.7355	HOMO-2 → LUMO 71%	0.82
	665.94	0.5493	HOMO-1 → LUMO 97%	0.72
	715.95	0.0028	HOMO → LUMO 100%	**0.01**

Values in bold represents the significant LHE values.

Table 4. Electronic properties of optimized P2 using 6-31G*, 6-31G** and 6–31 + G* basis set in gas phase.

Basis set	HOMO (eV)	LUMO (eV)	E_g (eV)	λ_{max} (nm)
6-31G*	-4.83	-2.97	1.86	750.98
6-31G**	-4.82	-2.97	1.85	752.30
6-31 + G*	-5.11	-3.28	1.83	767.79

$$J_{sc} = e\int LHE(\lambda).\ \Phi_{inj.}\ \eta_{reg.}\ \eta_{cc}\ I_s\ (\lambda)\ d\lambda \quad (4)$$

The J_{sc} is calculated by the LHE of dye, Φ_{inj}. η_{reg}. and η_{cc}. where Φ_{inj} = the quantum yield of charge injection from the excited dye into the TiO_2 conduction band, η_{reg} = the efficiency of regeneration, and η_{cc} = the charge collection efficiency [7].

LHE or absorptance plays a vital role in photoexcitation and photoconversion efficiency [59]. So, LHE for the optimized dyes are expressed as Eq. (5) [9, 10, 11, 12];

$$LHE = 1-10^{-f} \quad (5)$$

where f is the oscillator strength of the excited state associated with absorption wavelength [18,26].

High LHE is suitable to increase the photocurrent response through intramolecular charge transfer [60]. The LHE values of the simulated dyes are 0.70, 0.68, 0.65, 0.68, 0.70, 0.68, 0.65 and 0.01 (P1 to P8 respectively) as reported in Table 5. We observed that P1 and P5 with the highest value of oscillator strength exhibited the highest value (0.70) of LHE. Considering the effect of donor subunit, pyrrole broadens the absorption band compared to other simulated dyes hence improves LHE.

The V_{oc} measures the difference between the quasi-Fermi level of the electron in the TiO_2 conduction band and the redox potential of electrolyte [64,65]. High V_{oc} value reveals slower recombination of charges [65]. The V_{oc} of a photovoltaic cell is mainlyassociated with the LUMOs and conduction band of TiO_2 semiconductor [66]. Thus, V_{oc} is elucidated as Eq. (6) [67]:

$$V_{oc} = E_{LUMO} - E_{CB}^{TiO_2} \quad (6)$$

The calculated value for V_{oc} values for the dye ranges from 0.95 to 1.06 eV as shown in Table 5. It is obvious from the V_{oc} value of P1–P4 that higher LUMOs energy leads to an increase in V_{oc} value which is crucial to the greater photocurrent conversion efficiency of the DSSCs. P1 and P2 has the same value of V_{oc}, so also P3 and P4. Since the latter have unfavorable HOMO energies, then only P1 and P2 are considered as promising sensitizers that would exhibit better photocurrent conversion efficiency compared to other dyes. The variation of the V_{oc} values can also be associated with the effect of various incorporated donor subunit. Since a high V_{oc} value is better for a specific sensitizer, P2 with a V_{oc} value of 1.03 eV combined with its other attractive characteristics would have the best performance in DSSC amongst these dyes. Therefore, 2-hexylthiophene can be said to have a positive impact on the V_{oc} value of the simulated dye which can be attributed to the higher LUMO level of P2 dye.

3.7. Chemical reactivity parameters

Calculation of chemical reactivity parameters is relevant to understand the behavioral profiles of molecules in the environment. The chemical reactivity parameters of P3 and P4 were not reported due to their unmatched HOMO energies which is a pointer to poor photovoltaic performance. Calculations of the chemical reactivity parameters can be obtained from ionization potential (I) and electron affinity (A) [58]. Ionization potential shows the energy needed for electron removal from an isolated atom or ion in gaseous state while electron affinity investigates the energy emanating from addition of electron to an atom in gaseous state. These two parameters are used in calculation of chemical hardness as in Eq. (7) [43,44].

$$\eta = I - A \quad (7)$$

The electrophilicity index (ω) is calculated following the method reported by Parr et al. [68]. Thus, ω can be expressed as in Eq. (8) [43]:

$$\omega = \frac{(I+A)^2}{8\eta} \quad (8)$$

According to Gazquez et al. [69] and Zhao et al. [70], electrodonating power (ω^-) and electroaccepting power (ω^+) of a molecule can be determined following Eqs. (9) and (10) respectively;

$$\omega^- = \frac{(3I+A)^2}{16\eta} \quad (9)$$

$$\omega^+ = \frac{(I+3A)^2}{16\eta} \quad (10)$$

Chemical hardness is germane to understand resistance to charge transport in a chemical system [5]. The η values of all the optimized dyes are listed in Table 6. The dye used for DSSC should exhibit a low value of η to generate better short-circuit current density which results in excellent photoelectric conversion efficiency [71]. The calculated η values for P1, P2 and P5–P8 ranges from 3.83 to 4.09 eV P1, P5 and P7 have the same HOMO-LUMO gap (1.97 eV) but different values of η. This explains the effects of the donor subunit on the systems. It is also deduced that carbazole lowers resistance to charge transfer better than pyrrole. Similarly, the effect of an additional donor subunit to P6 and P8 containing indole and phenothiazine is better appreciated considering their η value. The two dyes also have the same energy gap (1.95 eV) but different η values due to the different chemical groups attached at the C7 point of the molecules. The charge transfer sequence is P2<P8<P7<P6<P5<P1. P2 has the lowest value of η (3.83 eV) and the lowest favourable energy gap (1.85 eV). It is expected that P2 would have better resistance to intramolecular charge transfer due to its low η value which can be attributed to the good structural stability of the sulphur atom on 2-hexylthiophene. Looking at the relationship between chemical hardness and energy gap in Figure 6, it can be concluded that chemical hardness is directly proportional to the HOMO-LUMO gap. Low chemical hardness and high LHE is significant for effective charge transfer and the better dye sensitizer [31]. So P2 is expected to perform better as a good sensitizer in the photovoltaic cell.

Electrophilicity index (ω) reveals the stabilization energy of the system in the process of getting more electrons from the external medium. The stabilization energy sequence is P1<P2<P5<P6<P7<P8 as shown in Table 6. We observed that nitrogen-containing donor subunits tend toward better stabilization energy. As reported by Domingo et al. [72] organic systems are classified as strong electrophiles when it has a value greater than 1.5 eV and moderate when its value ranges from 0.8 to 1.5 eV while regarded as marginal, when its value is below 0.8 eV. Interestingly, all the molecules are classified as strong electrophiles with P8 showing a high propensity of stability when an additional electron is being acquired from the environment. However, P1 is observed to exhibit low stabilization energy due to the absence of extended conjugation.

Table 5. Electronic properties of the studied dyes.

Dye	HOMO-1 (eV)	HOMO (eV)	LUMO (eV)	LUMO+1 (eV)	E_g (eV)	LHE	V_{oc} (eV)
P1	-5.82	-4.94	-2.97	-2.25	1.97	0.70	1.03
P2	-5.71	-4.82	-2.97	-2.25	1.85	0.68	1.03
P3	-5.62	-4.74	-2.94	-2.24	1.80	0.65	1.06
P4	-5.69	-4.79	-2.94	-2.24	1.85	0.68	1.06
P5	-5.75	-4.97	-3.00	-2.29	1.97	0.70	1.00
P6	-5.55	-4.97	-3.02	-2.31	1.95	0.68	0.98
P7	-5.52	-5.00	-3.03	-2.30	1.97	0.65	0.97
P8	-5.14	-5.00	-3.05	-2.33	1.95	0.01	0.95

Table 6. Molecular Descriptor Parameters of the studied dyes obtained by density functional theory (DFT) conceptual at B3LYP/6-31G** level of theory.

Dye	η (eV)	Ω (eV)	ω^- (eV)	ω^+ (eV)
P1	4.09	1.93	6.11	2.13
P2	3.83	1.96	6.10	2.22
P5	3.99	1.97	6.17	2.21
P6	3.93	1.99	6.20	2.25
P7	3.90	2.01	6.24	2.28
P8	3.88	2.02	6.26	2.30

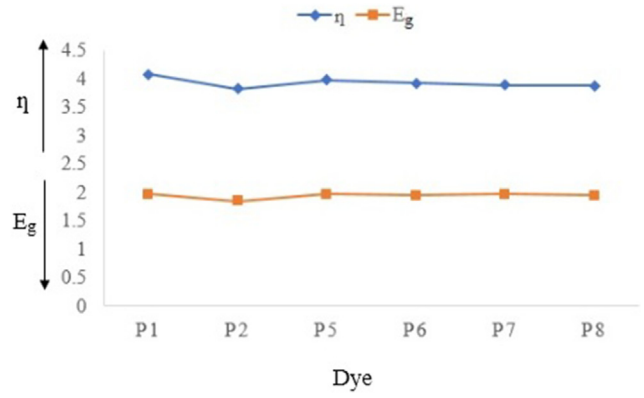

Figure 6. Relationship between chemical hardness and HOMO-LUMO energy gap of simulated dyes.

The electrodonating power (ω^-) has been described as the ability of a molecule to release electron whereas electroaccepting power (ω^+) show the electron acceptor capability of a molecule [71]. A smaller value of ω^- of a system makes it a better donor of electron density while a greater ω^+ value corresponds to a better capability of accepting electron density. ω^- and ω^+, ranges from 6.10 to 6.26 eV and 2.21–2.30 eV respectively as revealed in Table 6. P2 containing 2-hexylthiophene as donor subunit has the best electron donating capacity among others. P8 containing phenothiazine attachment exhibit highest electroaccepting power.

From the calculated properties for all the simulated dyes, the most preferred dye for photovoltaic cell among the optimized dyes is P2 due to low HOMO-LUMO gap, high absorption wavelength, low chemical hardness and high V_{oc} which is a pointer to high DSSC conversion efficiency.

4. Conclusion

New phenoxazine-based D-A_2-π-A_1 dyes, P1 to P8 have been theoretically investigated. Different donor subunits were introduced at C7 point of phenoxazine based dye skeleton. The donor subunits showed great influence on the electronic and absorption properties of the studied dyes. The LUMO values of all the optimized dyes are sufficiently greater than the conduction band of TiO_2 (-4.0 eV) and the HOMO levels are lower than the redox potential of I^-/I_3 electrolyte (-4.8 eV) except for P3 and P4 with unfavorable HOMO value (-4.74 and -4.79 eV) for electron regeneration with I^-/I_3 electrode. Hence, P3 and P4 are expected to show poor photovoltaic performance. Attachment of the donor subunits extended the π-conjugation, thus promoting intramolecular charge transfer and bathochromic shift. The introduction of 2-hexylthiophene in P2 significantly lowered the E_g and chemical hardness and produced good LHE. P2 is expected to have the best photovoltaic performance due to its competing electronic and absorption properties.

Declarations

Author contribution statement

Samson Olusegun Afolabi: Performed the experiments; Analyzed and interpreted the data; Wrote the paper.

Banjo Semire: Analyzed and interpreted the data; Contributed reagents, materials, analysis tools or data.

Mopelola Abidemi Idowu: Conceived and designed the experiments; Analyzed and interpreted the data; Wrote the paper.

Funding statement

This research did not receive any specific grant from funding agencies in the public, commercial, or not-for-profit sectors.

Data availability statement

Data included in article/supplementary material/referenced in article.

Declaration of interests statement

The authors declare no conflict of interest.

Additional information

Supplementary content related to this article has been published online at https://doi.org/10.1016/j.heliyon.2021.e06827.

Acknowledgements

The contributions of staff from the Department of Chemistry, Federal University of Agriculture, Abeokuta, Ogun State, Nigeria are well appreciated. Authors thank the Department of Pure and Applied Chemistry, LAUTECH, Ogbomoso for the provision of facilities to carry out the research.

References

[1] E.J. Hoevenaars, C.A. Crawford, Implications of temporal resolution for modeling renewables-based power systems, Renew. Energy 41 (2012) 285–293.
[2] K.M. Haradhan, Acid rain is a local environment pollution but global concern, Open Sci. J. Analyt. Chem. 3 (2018) 47–55.
[3] P. Frederica, Pollution from fossil-fuel combustion is the leading environmental threat to global pediatric health and equity solutions exist, Int. J. Environ. Res. Publ. Health 15 (1) (2018) 16 (17 pages).
[4] H. Kafafy, H. Wu, M. Peng, H. Hu, K. Yan, R.M. El-Shishtawy, D. Zou, Steric and solvent effect in dye-sensitized solar cells utilizing phenothiazine-based dye, Int. J. Photoenergy (2014) 1–9.
[5] C. Sun, Y. Li, P. Song, F. Ma, An experimental and theoretical investigation of the electronic structures and photoelectrical properties of ethyl red and carminic acid for DSSC application, Materials 9 (2016) 813 (22 pages).
[6] B. O'Regan, M. Grätzel, A low-cost, high-efficiency solar cell based on dye-sensitized colloidal titanium dioxide films, Nature 353 (1991) 737–740.
[7] B. Semire, A. Oyebamiji, O.A. Odunola, Electronic properties' modulation of D–A–A via fluorination of 2-cyano-2-pyran-4-ylidene-acetic acid acceptor unit for efficient DSSCs: DFT-TDDFT approach, Scientif. Afr. 7 (2020), e00287 (10 pages).
[8] F. Arkan, M. Izadyar, The investigation of the central metal effects on the porphyrin-based DSSCs performance; molecular approach, Mater. Chem. Phys. 196 (2017) 142–152.
[9] I.N. Obotowo, I.B. Obot, U.J. Ekpe, Organic sensitizers for dye-sensitized solar cell (DSSC): properties from computation, progress and future perspectives, J. Mol. Struct. 1122 (2016) 80–87.
[10] Y. Hua, Design and synthesis of new organic dyes for highly efficient dye-sensitized solar cells (DSSCs), J. Power Sources 243 (2014) 253–259.
[11] J.J. Fu, Y.A. Duan, J.Z. Zhang, M.S. Guo, Y. Liao, Theoretical investigation of novel phenothiazine-based D-π-A conjugated organic dyes as dye-sensitizer in dye-sensitized solar cells, Comput. Theoret. Chem. 1045 (2014) 145–153.
[12] C.V. Kumar, D. Raptis, E.N. Koukaras, L. Sygellou, P. Lianos, Study of an indoline–phenothiazine based organic dye for dye-sensitized solar cells. Theoretical calculations and experimental data, Org. Electron. 25 (2015) 66–73.
[13] M. Li, L. Kou, L. Diao, Q. Zhang, Z. Li, Q. Wu, W. Lu, D. Pan, Theoretical study of acene-bridged dyes for dye-sensitized solar cells, J. Phys. Chem. 119 (13) (2015) 3299–3309.
[14] X. Zhang, F. Gou, J. Shi, H. Gao, Z. Zhu, H. Jing, Molecular engineering of new phenothiazine-based D-A-π-A dyes for dye-sensitized solar cells, RSC Adv. 6 (108) (2016) 106380–106386.
[15] Y. Hua, S. Chang, D. Huang, X. Zhou, X. Zhu, J. Zhao, T. Chen, W.Y. Wong, Significant improvement of dye-sensitized solar cell performance using simple phenothiazine-based dyes, Chem. Mater. 25 (10) (2013) 2146–2153.
[16] D. Kim, J.K. Lee, S.O. Kang, J. Ko, Molecular engineering of organic dyes containing N-aryl carbazole moiety for solar cell, Tetrahedron 63 (2007) 1913–1922.
[17] K.D. Seo, I.T. Choi, Y.G. Park, S. Kang, J.Y. Lee, H.K. Kim, Novel D-A-π-A coumarin dyes containing low band-gap chromophores for dye-sensitized solar cells, Dyes Pigments 94 (2012) 469–474.
[18] Y. Wu, M. Marszalek, S.M. Zakeeruddin, Q. Zhang, H. Tian, M. Gratzel, W. Zhu, High-conversion-efficiency organic dye-sensitized solar cells: molecular engineering on D-A-π-A featured organic indoline dyes, Energy Environ. Sci. 5 (2012) 8261–8272.
[19] C. Li, J.H. Yum, S.J. Moon, A. Herrmann, F. Eickemeyer, N.G. Pschirer, P. Erk, J. Schöneboom, K. Mullen, M. Gratzel, M.K. Nazeeruddin, An improved perylene sensitizer for solar cell applications, ChemSusChem 1 (2008) 615–618.
[20] Z. Wan, C. Jia, Y. Duan, X. Chen, Z. Li, Y. Lin, Novel organic sensitizers containing dithiafulvenyl units as additional donors for efficient dye-sensitized solar cells, RSC Adv. 4 (2014) 34896–34903.
[21] B. Peng, S. Yang, L. Li, F. Cheng, J.A. Chen, Density functional theory, andtime-dependent density functional theory investigation on the anchor comparison of triarylamine-based dyes, J. Chem. Phys. 132 (2010) 34305–34309.
[22] H. Tian, X. Yang, J. Pan, R. Chen, M. Liu, Q. Zhang, A. Hagfeldt, L. Sun, A triphenylamine dye model for the study of intramolecular energy transfer and charge transfer in dye sensitized solar cells, Adv. Funct. Mater. 18 (2008) 3461–3468.
[23] U. Mehmood, I.A. Hussein, K. Harrabi, S. Ahmed, Density functional theory study on the electronic structures of oxadiazole based dyes as photosensitizer for dye sensitized solar cells, Advances in Materials Science and Engineering 2015 (2015) 1–8.
[24] H. Tan, C. Pan, G. Wang, Y. Wu, Y. Zhang, G. Yu, M. Zhang, A comparativestudy on properties of two phenoxazine-based dyes for dye-sensitized solar cells, Dyes Pigments 101 (2014) 67–73.
[25] Z.J. Chermahini, A.N. Chermahini, Theoretical study on the bridge comparison of TiO_2 nanoparticle sensitizers based on phenoxazine in dye-sensitized solar cells, Theor Chem Acc 136 (2017) 34 (10 pages).
[26] K.M. Karlsson, X. Jiang, S.K. Eriksson, E. Gabrielsson, H. Rensmo, A. Hagfeldt, L. Sun, Phenoxazine dyes for dye-sensitized solar cells: relationship between molecular structure and electron lifetime, Chemistry-A Eu. J. 17 (2011) 6415–6424.
[27] W. Lee, S.B. Yuk, J. Choi, H.J. Kim, H.W. Kim, S.H. Kim, B. Kim, M.J. Ko, J.P. Kim, The effects of the number of anchoring groups and N-substitution on the performance of phenoxazine dyes in dye-sensitized solar cells, Dyes Pigments 102 (2014) 13–21.
[28] Y. Numata, A. Islam, H. Chen, L. Han, Aggregation-free branch-type organic dye with a twisted molecular architecture for dye-sensitized solar cells, Energy Environ. Sci. 5 (9) (2012) 8548–8552.
[29] N. Instroza, F. Mendizabal, P.R. Arratia, C. Orellana, F.C. Linares, Improvement of photovoltaic performance by substituent effect of donor and acceptor structure of TPA-based dye-sensitized solar cell, J. Mol. Model. 22 (2016) 25 (7 pages).
[30] M. Cariello, S.M. Abdalhadi, P. Yadav, J.D. Decoppet, S.M. Zakeeruddin, M. Gratzel, A. Hagfeldt, G. Cooke, An investigation of the roles furan versus thiophene π-bridges play in donor-π-acceptor porphyrin based, DSSCs Dalton Trans 47 (2018) 6549–6556.
[31] B. Semire, A. Oyebamiji, O.A. Odunola, Tailoring of energy levels in (2Z)-2-cyano-2-[2-[(E)-2-[2-[(E)-2-(ptolyl)vinyl]thieno[3,2-b]thiophen-5-yl]vinyl]pyran-4-ylidene]acetic acid derivatives via conjugate bridge and fluorination of acceptor units for effective D–π–A dye-sensitized solar cells: DFT–TDDFT approach, Res. Chem. Intermed. 43 (2017) 1863–1879.
[32] A.F. Buene, N. Boholm, A. Hagfeldt, B.H. Hof, Effect of furan p-spacer and triethylene oxide methyl ether substituents on performance of phenothiazine sensitizers in dye-sensitized solar cells, New J. Chem. 43 (2019) 9403–9410.
[33] A. Hagfeldt, G. Boschloo, L. Sun, L. Kloo, H. Pettersson, Dye-sensitized solar cells, Chem. Rev. 110 (11) (2010) 6595–6663.
[34] C.H. Liu, R. Niazi, D.F. Perepichka, Extraordinary enhancement of π-electron donor/acceptor ability by DD/AA complementary hydrogen bonding, Angew. Chem. Int. Ed. 58 (2019) 2–11.
[35] L. Zheng, Q. Cao, J. Wang, Z. Chai, G. Cai, Z. Ma, H. Han, Q. Li, Z. Li, H. Chen, Novel D–a–π–A-type organic dyes containing a ladderlike dithienocyclopentacarbazole donor for effective dye-sensitized solar cells, ACS Omega 2 (2017) 7048–7056.
[36] T. Suresh, R.K. Chitumalla, N.T. Hai, J. Jang, T.J. Lee, J.H. Kim, Impact of neutral and anion anchoring groups on the photovoltaic performance of triphenylamine sensitizers for dye-sensitized solar cells, RSC Adv. 6 (2016) 26559–26567.
[37] Y. Li, C. Sun, D. Qi, P. Song, F. Ma, Effects of different functional groups on the optical and charge transport properties of copolymers for polymer solar cells, RSC Adv. 6 (2016) 61809–61820.
[38] S. Feng, Q.S. Li, L.N. Yang, Z.Z. Sun, T.A. Niehaus, Z.S. Li, Insights into aggregation effects on optical property and electronic coupling of organic dyes in dye sensitized solar cells, J. Power Sources 273 (2015) 282–289.
[39] M.K. Nazeeruddin, F. De-Angelis, S. Fantacci, A. Selloni, G. Viscardi, P. Liska, S. Ito, T. Bessho, M. Grätzel, Combined experimental and DFT/TDDFT computational study of photoelectrochemical cell ruthenium sensitizers, J. Am. Chem. Soc. 127 (48) (2005) 16835–16847.
[40] C. Lee, W. Yang, R.G. Parr, Development of the Colle-Salvetti correlation-energy formula into a functional of the electron density, Phys. Rev. 37 (2) (1988) 785–789.
[41] D. Jacquemin, E.A. Perpete, I. Ciofini, C. Adamo, Accurate simulation of optical properties in dyes, Acc. Chem. Res. 42 (2009) 326–334.
[42] W. Fan, Y.Z. Chang, J.L. Zhao, Z.N. Xu, D.Z. Tan, Y. Chen, Theoretical study of fused thiophene modified anthracene-based organic dyes for dye-sensitized solar cells applications, New J. Chem. 42 (2018) 20163–20170.
[43] T. Delgado-Montiel, J. Baldenebro-López, R. Soto-Rojo, D. Glossman-Mitnik, Quantum chemical study of the effect of π-bridge on the optical and electronic properties of sensitizers for DSSCs incorporating dioxythiophene and thiophene units, Theor. Chem. Acc. 135 (10) (2016) 235 (10 pages).
[44] T. Delgado-Montiel, J. Baldenebro-López, R. Soto-Rojo, D. Glossman-Mitnik, Theoretical study of the effect of π-bridge on optical and electronic properties of carbazole-based sensitizers for DSSCs, Molecules 25 (2020) 3670 (17 pages).
[45] M. Bourass, A.T. Benjelloun, M. Hamidi, M. Benzakour, M. Mcharfi, M. Sfaira, S. F Serein, J.P. Le re-Porte, J.M. Sotiropoulos, S.M. Bouzzine, M. Bouachrine, J. Saudi, DFT theoretical investigations of p-conjugated molecules based on thienopyrazine and different acceptor moieties for organic photovoltaic cells, J. Saudi Chem. Soci. 20 (2013) 415–425.
[46] T. Lu, F. Chen, Multiwfn: a multifunctional wavefunction analyzer, J. Comput. Chem. 33 (2012) 580–592.
[47] A. Mohajeri, A. Omidvar, H. Setoodeh, Fine structural tuning of thieno[3,2-b] pyrrole donor for designing banana-shaped semiconductors relevant to organic field effect transistors, J. Chem. Inf. Model. 59 (5) (2019) 1930–1945.
[48] Spartan 14, Wavefunction, INC, Irvine CA 92612, USA.
[49] P. Prajongtat, S. Suramitr, S. Nokbin, K. Nakajima, K. Mitsuke, S. Hannongbua, Density functional theory study of adsorption geometries and electronic structures of azo-dye-based molecules on anatase TiO2 surface for dye-sensitized solar cell applications, J. Mol. Graph. Model. 76 (2017) 551–561.
[50] H. Terasaki, D.J. Frost, D.C. Rubie, F. Langenhorst, The effect of oxygen and sulphur on the dihedral angle between Fe–O–S melt and silicate minerals at high pressure: implications for Martian core formation, Earth Planet Sci. Lett. 232 (3-4) (2005) 379–392.
[51] S. Jungsuttiwong, R. Tarsang, T. Sudyoadsuk, V. Promarak, P. Khongpracha, S. Namuangruk, Theoretical study on novel double donor-based dyes used in high efficient dye-sensitized solar cells: the application of TDDFT study to the electron injection process, Org. Electron. 14 (2013) 711–722.
[52] R.M. El-shishtawy, M.A. Abdullah, G.A. Saadullah, A.K.E. Shaaban, Molecular design of donor-acceptor dyes for efficient dye-sensitized solar cells I: a DFT study, J. Mol. Model. 20 (6) (2014) 2241–2245.

[53] W. Fan, W.Q. Deng, Incorporation of thiadiazole derivatives as π-spacer to construct efficient metal-free organic dye sensitizers for dye-sensitized solar cells: a theoretical study, Commun. Comput. Chem. 1 (2) (2013) 152–170.
[54] I.V. Alabugin, S. Bresch, M. Manoharan, Hybridization trends for main group elements and expanding the bent's rule beyond carbon: more than electronegativity, J. Phys. Chem. 118 (20) (2014) 3663–3677.
[55] C. Theivarasua, R. Murugesan, Natural bond orbital (NBO) population analysis of an energetic molecule 1-phenyl-2- nitroguanidine, Int. J. Chem. Sci. 14 (4) (2016) 2029–2050.
[56] N. Bouzayen, M. Mbarek, K. Alimi, Solvent effects on optical and electronic properties of carbazole benzothiazole based bipolar compound: TD-DFT/PCM approach, Comput. Theor. Chem 3 (1) (2015) 28–39.
[57] M.D. Kumar, P. Rajesh, R.P. Dharsini, M.E. Inban, Molecular geometry, NLO, MEP, HOMO-LUMO and mulliken charges of substituted piperidine phenyl hydrazines by using density functional theory, Asian J. Chem. 32 (2020) 401–407.
[58] M. Raftani, T. Abram, M.N. Bennani, M. Bouachrine, Theoretical study of new conjugated compounds with a low bandgap for bulk heterojunction solar cells: DFT and TD-DFT study, Results in Chemistry 2 (2020) 100040 (12 pages).
[59] M. Katono, M. Wielopolski, M. Marszalek, T. Bessho, J.E. Moser, R. Humphry-Baker, S.M. Zakeeruddin, M. Gratze, Effect of extended π-conjugation of the donor structure of organic D–a—π–A dyes on the photovoltaic performance of dye-sensitized solar cells, J. Phys. Chem. C 118 (30) (2014) 16486–16493.
[60] S.O. Afolabi, B. Semire, O.K. Akiode, T.A. Afolabi, G.A. Adebayo, M.A. Idowu, Design and theoretical study of phenothiazine-based low bandgap dye derivatives as sensitizers in molecular photovoltaics, Opt. Quant. Electron. 52 (2020) 476 (18 pages).
[61] H. Tian, X. Yang, J. Cong, R. Chen, C. Teng, J. Liu, Y. Hao, L. Wang, L. Sun, Effect of different electron donating groups on the performance of dye-sensitized solar cells, Dyes Pigments 84 (2010) 62–68.
[62] A. Fitri, A.T. Benjelloun, M. Benzakour, M. McHarfi, M. Hamidi, M. Bouachrine, Theoretical investigation of new thiazolothiazole-based D-π-A organic dyes for efficient dye-sensitized solar cell, Spectrochim. Acta Part A Mol. Biomol. Spectrosc. 124 (2014) 646–654.
[63] H. Wang, B. Wang, J. Yu, Y. Hu, C. Xia, J. Zhang, R. Liu, Significant enhancement of power conversion efficiency for dye sensitized solar cell using 1D/3D network nanostructures as photoanodes, Sci. Rep. 5 (2015) 9305 (9 pages).
[64] Y. Wu, W. Zhu, Organic sensitizers from D–π–A to D–A–π–A: effect of the internal electron-withdrawing units on molecular absorption, energy levels and photovoltaic performances, Chem. Soc. Rev. 42 (5) (2013) 2039–2058.
[65] N.A. Wazzan, A DFT/TDDFT investigation on the efficiency of novel dyes with ortho-fluorophenyl units (A1) and incorporating benzotriazole/benzothiadiazole/phthalimide units (A2) as organic photosensitizers with D–A2–π–A1 configuration for solar cell applications, J. Comput. Electron. 18 (2019) 375–395.
[66] A. Arunkumar, S. Shanavas, R. Acevedo, P.M. Anbarasan, Computational analysis on D–π–A based perylene organic efficient sensitizer in dye-sensitized solar cells, Opt. Quant. Electron. 52 (3) (2020) 164 (13 pages).
[67] W. Sang-aroon, S. Saekow, V. Amornkitbamrung, J. Photochem. Photobiol, A Density functional theory study on the electronic structure of Monascus dyes as photosensitizer for dye-sensitized solar cells, J. Photochem. Photobiol. Chem. 236 (2012) 35–40.
[68] R.G. Parr, L. Szentpaly, S. Liu, Electrophilicity index, J. Am. Chem. Soc. 121 (9) (1999) 1922–1924.
[69] J.L. Gazquez, A. Cedillo, A. Vela, Electrodonating and electroaccepting powers, J. Phys. Chem. 111 (2007) 1966–1970.
[70] D. Zhao, Q. Lu, R. Su, Y. Li, M. Zhao, Light harvesting and optical-electronic properties of two quercitin and rutin natural dyes, Appl. Sci. 9 (2019) 2567 (17 pages).
[71] T. Delgado-Montiel, R. Soto-Rojo, J. Baldenebro-López, D. Glossman-Mitnik, Theoretical study of the effect of different π bridges including an azomethine group in triphenylamine-based dye for dye-sensitized solar cells, Molecules 24 (2019) 3897 (16 pages).
[72] L.R. Domingo, M. Ríos-Gutiérrez, P. Pérez, Applications of the conceptual density functional theory indices to organic Chemistry reactivity, Molecules 21 (6) (2016) 748 (22 pages).